Column-V acceptors in ZnSe

K. W. Kwak, R. D. King-Smith, and David Vanderbilt

Department of Physics and Astronomy, Rutgers University, Piscataway, New Jersey 08855-0849

The structural and electronic properties of substitutional phosphorus and nitrogen impurities in ZnSe are studied using pseudopotential total-energy calculations. Substitutional phosphorus and nitrogen, in their neutral states, form shallow acceptors. In the case of phosphorus, the symmetry is lowered from T_d to C_{3v} by a Jahn-Teller distortion, and the hole is more localized on the phosphorus site. For nitrogen, however, the Jahn-Teller distortion is so small that the symmetry is approximately T_d, and the hole density is spread around nearby selenium-atom sites. For nitrogen in the positive charge state, two minimal-energy configurations are predicted: a stable state with approximately T_d symmetry and a metastable state with C_{3v} symmetry, which is 0.3 eV higher in energy than the stable one.

I. INTRODUCTION

Wide-band-gap II-VI compounds form an important class of semiconducting materials, especially in view of their promise for applications in optoelectronic devices. For example, the band gap of ZnSe, 2.67 eV at room temperature, makes it suitable for construction of a blue light-emitting laser diode. However, the fabrication of p-n heterojunctions in ZnSe has been hindered by doping difficulties: ZnSe is easily doped n type, but is difficult to dope p type. Both column-I and column-V elements have been widely employed as p-type dopants, but low-resistivity p-type ZnSe has been obtained only with Li and N. For N doping, a net acceptor concentration $(N_A - N_D)$ of 1.0 $\times 10^{18}$ has recently been achieved in ZnSe grown by molecular-beam epitaxy (MBE) using an active nitrogen beam generated by a free radical source.[1] Using this technology, blue-green diode lasers have been fabricated from II-VI materials.[2]

In spite of this success in fabricating low-resistivity p-type ZnSe using nitrogen as the dopant, the origin of the doping difficulties remains unclear. While several explanations have been suggested,[3–8] there is no firm evidence for any of them. The most commonly accepted explanation is that native defects (e.g., Se vacancies or Zn interstitials) which act as donors are activated as a result of the doping, resulting in compensation of the acceptor impurities. Defect formation is energetically favorable since, due to the wide band gap, the energy needed to form a native donor defect can be balanced by the recombination energy of electrons at defect levels in the gap with the holes at the Fermi level. However, Laks and Van de Walle[6] employed *ab initio* total-energy calculations to investigate self-compensation by native defects in ZnSe, and suggested that native-defect concentrations in stoichiometric ZnSe were too low to cause compensation. Deviations from stoichiometry in ZnSe can produce large numbers of native defects; however, this is also true for GaAs, which can be doped p type without compensation by the native defects. Also, this mechanism would predict the impossibility of p-type doping regardless of dopant, which seems inconsistent with the success of p-type doping of ZnSe using N. Thus the native-defect self-compensation mechanism alone probably cannot explain the doping problem. Solubility limitations may play a role in the case of some dopants, especially alkalis,[6] but seem less plausible for column-V dopants. Another plausible explanation is dopant self-compensation, that is, transformation of the dopant into a deep center by large lattice relaxation.[7]

The fact that low-resistivity p-type ZnSe has been fabricated successfully using nitrogen doping, despite the failure with other column-V dopants such as phosphorus and arsenic, suggests that comparing the electronic properties of nitrogen and phosphorus impurities in ZnSe might lead to a better understanding of the doping problem. For nitrogen substituted on a selenium site in ZnSe, only one ionization energy of about 110 meV is known,[9] suggesting that substitutional nitrogen forms a shallow acceptor. However, for substitutional phosphorus on a selenium site, two kinds of ionization energies have been reported.[10] One is a deep center with an ionization energy of 0.6–0.7 eV,[11–13] and the other is a shallow acceptor at about 90 meV.[9,14] Based on electron paramagnetic resonance (EPR) and other optical experiments on phosphorus-doped ZnSe, Watts and co-workers[11,12] ascribed the deep center to a phosphorus ion substituted at a selenium site with a large associated Jahn-Teller distortion. The symmetry was identified to be C_{3v}, lowered from T_d symmetry of the host material by the distortion. This transformation of a shallow acceptor into a deep center is an example of a self-compensation process which could help explain the difficulties with p-type doping.

In this paper we employed pseudopotential total-energy calculations to study nitrogen and phosphorus impurities substituting on the selenium site in ZnSe, in the neutral, -1, and $+1$ charge states. For each state, we calculated the forces acting on the ions, and relaxed the ionic positions using the forces to obtain the stable struc-

ture of the system, assuming C_{3v} symmetry. The result of our calculation shows that nitrogen substituted on a selenium site, in its neutral state, forms a shallow acceptor, in a good agreement with experiments. Its stable structure has very nearly the original T_d symmetry of the host ZnSe. For substitutional phosphorus, in its neutral state, we find a shallow acceptor state whose ionization energy is $\lesssim 100$ meV. It has a C_{3v}-symmetry configuration, lowered from T_d symmetry due to a Jahn-Teller distortion. However, we did not find the deep state suggested by Watts et al. The implication of this discrepancy is discussed in detail in later sections.

The manuscript is organized as follows. In Sec. II, we briefly describe the calculational method. In Sec. III, we present the calculations of structural parameters of bulk ZnSe. The agreement with the experimental data is very good, showing that our calculational method is reliable. In Sec. IV, we present the results of defect calculations. We first discuss the choice of 32-atom supercell we use in the defect calculations. We then describe the structural and electronic properties of phosphorus and nitrogen defects. In Sec. V, we discuss the results of defect calculations and compare the results with various experiments on phosphorus and nitrogen dopants in ZnSe. Then we summarize in Sec. VI.

II. METHOD OF CALCULATION

In this section we describe the theoretical methods used to study the energetics and the electronic properties of bulk and defected ZnSe. An accurate and efficient *ab initio* theoretical approach to the study of defected ZnSe should (i) allow for the calculation of forces on atoms, in order to obtain relaxed structures; (ii) avoid exceedingly large basis sets; and (iii) include the occupied cation d states of the II-IV host.

The highly localized $3d$ orbitals of Zn present a severe limitation on the use of traditional norm-conserving pseudopotential approaches using plane-wave basis sets. The norm-conserving condition, which requires that the total pseudocharge inside the core match that of the all-electron wave function, makes it impossible to construct a pseudo wave function that is much smoother than the all-electron one. The norm-conserving pseudo wave functions of the Zn $3d$ states require a large number of plane waves in the basis set. These Zn $3d$ states may be included in the core shell, but this results in a poor description of bulk ZnSe. For example, the previous works on ZnSe and ZnS have shown[15-17] that the inclusion of Zn $3d$ states in the core shell can lead to the errors on the order of 10% in the equilibrium lattice constant. If the $3d$ states are included in the valence shell, the accuracy becomes quite good [comparable to that of all-electron linear augmented-plane-wave (LAPW) calculations[17,18]], but at the expense of introducing such a large plane-wave cutoff (e.g., maximum kinetic energy of 121 Ry in Ref. 17) as to make supercell defect calculations very difficult. Moreover, the calculation of forces tends to be problematic in the all-electron approaches.

In this work, we employ a new plane-wave pseudopo-

tential approach to density-functional theory in the local-density approximation.[19-21] An unusual feature of our approach is the treatment of the occupied Zn $3d$ states in the *valence shell* using the ultrasoft pseudopotential scheme introduced recently by Vanderbilt.[19] The generalization of the norm-conservation constraint in this scheme allows us to soften the pseudopotential by moving the peak of Zn $3d$ pseudo-wave-function to larger r. In Fig. 1 we compare the form of the all-electron and pseudo wave functions for the Zn $3d$ states. It is readily verified that the pseudo wave function converges much more rapidly in reciprocal space than the all-electron wave function. Using the present scheme, we obtain good structural properties of bulk ZnSe with a plane-wave cutoff of only 25 Ry, yet we can still calculate forces on the atoms so as to relax atomic coordinates efficiently for the defect structures. For the case of nitrogen impurities, the problematic N p states can be treated as easily as those of the heavier column-V dopants within this scheme. For the exchange-correlation potential, we used the Ceperley-Alder form as parametrized by Perdew and Zunger.[22]

A preconditioned conjugate-gradient method[21] has been used to minimize the Kohn-Sham energy functionals at fixed ionic configurations. This method is similar to that introduced by Teter, Payne, and Allan,[23] but this version[21] (i) updates all bands and all **k** points simultaneously, and (ii) uses a generalized Kohn-Sham energy functional in the space of nonorthogonal orbitals.[24]

A 32-atom bcc supercell used in the defect calculation is shown in Fig. 2. The supercell contains the formula unit $Zn_{16}Se_{15}X$ per 32-atom cell ($X =$ N or P) to represent the isolated defect. We fixed the lattice constant of the cell to be the experimental one. The integration over the supercell Brillouin zone was approximated by a special[25] **k** point $\frac{2\pi}{b}(\frac{1}{2} \frac{1}{2} \frac{1}{2})$, where b is the lattice constant of the supercell (11.34 Å). For a system with C_{3v} geometry, the **k**-point set which is equivalent to the **k** point $\frac{2\pi}{b}(\frac{1}{2} \frac{1}{2} \frac{1}{2})$ for a system with T_d geome-
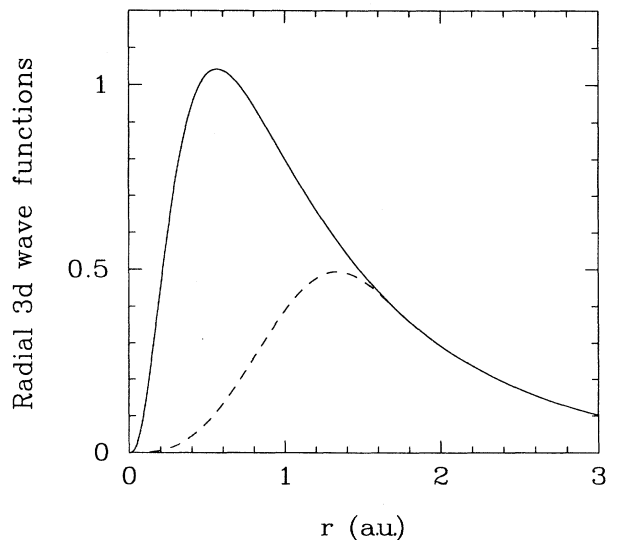

FIG. 1. All-electron (solid line) and pseudo- (dashed line) wave-function for $3d$ state of Zn.
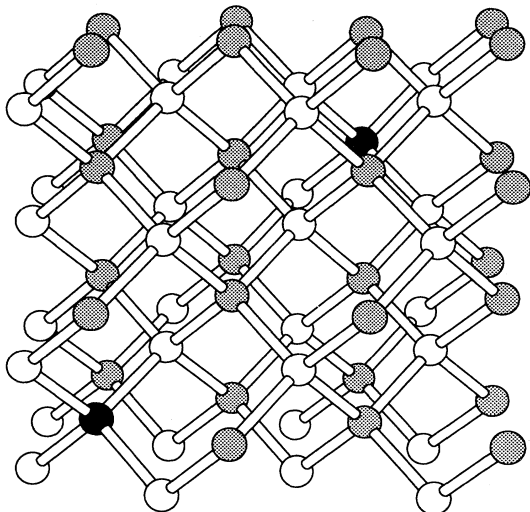
FIG. 2. 32-atom bcc structure used for defect calculations. Filled, shaded, and open atoms represent impurity, Se, and Zn atoms, respectively.

TABLE I. Comparison of calculated and experimental values of the lattice constant a, bulk modulus B_0, and zone-center TO phonon frequency $\omega_{TO}(\Gamma)$ of bulk ZnSe.

	a (Å)	B_0 (GPa)	$\omega_{TO}(\Gamma)$ (THz)
Calc.	5.60	67.7	5.96
Expt.	5.67[a]	62.5[b]	6.09[c]
Difference	−1.2%	8.2%	−2.1%

[a]Reference 27.
[b]Reference 34.
[c]Reference 35.

try is a set of two **k** points $\frac{2\pi}{b}(\frac{1}{2}\frac{1}{2}\frac{1}{2})$ with weight $\frac{1}{4}$, and $\frac{2\pi}{b}(-\frac{1}{2}\frac{1}{2}\frac{1}{2})$ with weight $\frac{3}{4}$. However, for the bcc cell the two **k** points are related by a reciprocal lattice vector $\frac{2\pi}{b}(100)$; thus only one **k** point was needed even for a system with C_{3v} geometry. When mapped into the bulk ZnSe irreducible Brillouin zone, our **k**-point mesh maps into a set of two **k** points, $\frac{2\pi}{a}(\frac{1}{4}\frac{1}{4}\frac{1}{4})$ with weight $\frac{1}{4}$ and $\frac{2\pi}{a}(\frac{3}{4}\frac{1}{4}\frac{1}{4})$ with weight $\frac{3}{4}$, where a is the lattice constant of bulk ZnSe (5.67 Å). Alternatively, our mesh can be viewed as equivalent to a single **k** point in the full Brillouin zone of a 64-atom supercell. Tests indicate that with this **k**-point set, the total energy is converged to better than 0.02 eV/atom.

To obtain the minimum-energy structure for each defect (for example, P_{Se}^0), we started with an arbitrary configuration of the ions in the cell. Using the conjugate-gradient minimization technique, the Kohn-Sham energy functional was minimized to obtain the electronic ground state for the fixed ionic configuration, and the forces on ions were calculated. Then, according to the forces, the ions in the unit cell were moved to decrease the forces. This procedure was repeated until the forces were negligible (less than 0.05 eV/Å). The modified Broyden scheme[26] was used in this relaxation procedure of ionic coordinates. In some cases, the ions were relaxed subject to a constraint on the length of a particular bond. In such cases, the ionic coordinates were relaxed until the only remaining forces were equal and opposite forces on the two atoms, directed along the bond.

III. STRUCTURAL PROPERTIES OF BULK ZnSe

To check the reliability of our calculational methods and pseudopotentials for Zn and Se, we calculated the equilibrium lattice constant, bulk modulus, and zone-center TO phonon frequency of bulk ZnSe. In the calcu-

lation, a set of ten special **k** points in the irreducible Brillouin zone was used. Table I shows the calculated bulk properties of ZnSe compared with experimental data. The level of agreement is typical of high-quality *ab initio* calculations on other semiconductor systems.

Our calculations correctly predict a direct band gap at the Γ point in the Brillouin zone of bulk ZnSe. The calculated value of the band gap is 1.37 eV, which is about half of the experimental value of 2.80 eV.[27] It is well known that the local-density approximation (LDA) predicts too small a band gap in the case of semiconductors since it does not describe properly the excited states of the system.[28]

IV. RESULTS OF DEFECT CALCULATIONS

A. Choice of supercell

Besides the 32-atom cell which was used in the present defect calculations, we tried two other supercells in preliminary calculations of neutral P_{Se}. One was an eight-atom simple-cubic cell containing Zn_4Se_3P per unit cell, and the other was a 16-atom fcc cell containing Zn_8Se_7P per unit cell. By the same procedure as will be described shortly for the 32-atom cell, we obtained the total energy for both the eight-atom and 16-atom cells as a function of the configuration coordinate Q describing the Jahn-Teller distortion. In these calculations, we used a special **k** point $\frac{2\pi}{a}(\frac{1}{4}\ \frac{1}{4}\ \frac{1}{4})$ for T_d geometries and the equivalent set of two **k** points for C_{3v} geometries. With this set of special **k** points, we obtained qualitatively similar plots of total energy as a function of Q for eight-atom and 16-atom cell calculations to that of 32-atom cell calculation. For example, the Q_m value of the relaxed Jahn-Teller distorted structure was 0.15 Å for the eight-atom calculation, compared to 0.17 Å for the 32-atom calculation. Thus, from the point of view of total energies, the supercell size seems to be well converged.

We have also carried out tests to check whether the supercells considered are large enough to represent the electronic structure of isolated impurities adequately. We calculated the band structure of a Jahn-Teller distorted configuration for each supercell to check whether the defect state has a sufficiently small dispersion. In the case of the eight-atom cell, we calculated the band structure along the line from Γ to $\frac{2\pi}{a}(\frac{1}{2}\ \frac{1}{2}\ \frac{1}{2})$, and, for 16-atom and

32-atom cells, along Γ to $\frac{2\pi}{a}$ ($\frac{1}{4}$ $\frac{1}{4}$ $\frac{1}{4}$), where a is the lattice constant of bulk ZnSe. The band dispersions of the defect states in these directions are about 1.8 eV and 1.5 eV for the eight-atom and 16-atom cells, respectively. With such a large dispersion, the defect-state bands cross some of the other valence bands, suggesting that the interactions between impurities in the neighboring cells are still rather strong. For the larger 32-atom cell, the dispersion of the defect level is 0.37 eV, quite small compared to those of the smaller cells, and the level crossing is absent. It was largely this analysis which convinced us to use the 32-atom supercell for all our final calculations.

The drastic decrease of the dispersion in the case of the 32-atom cell indicates the importance of the impurity-impurity interactions along the zigzag chains running in the [110] directions. In the case of the 16-atom cell, the interactions between an impurity atom and the nearest neighboring impurity in the [110] direction at a distance of $\sqrt{2}a$ are strong and important. In the 32-atom cell, the nearest-neighbor impurity atoms are in the [111] directions with a distance of $\sqrt{3}a$, and the corresponding strong interactions between the impurities in the [110] directions are absent. This explanation is consistent with previous work on tetrahedral semiconductors which revealed the importance of the interactions along the chains running in the [110] directions.[29,30]

B. Breathing relaxations

We now turn to the details of our calculations on defects in zinc selenide. We first used the calculated ionic forces to determine the breathing relaxations for N_{Se} and P_{Se} in their -1, 0, and $+1$ charge states in the 32-atom cell, by assuming retention of full tetrahedral T_d symmetry. The bond lengths between the impurities and the neighboring Zn atoms are shown in Table II. We found a substantial contraction relative to the ideal bond length of 2.45 Å, for the case of P and especially N. We also calculated the breathing relaxation for neutral P_{Se} in the 16-atom fcc supercell, and found a bond length of 2.34 Å, larger by only 0.01 Å, suggesting that the calculations are reasonably converged.

An interesting feature of the results in Table II is that, in going from the neutral to the -1 charge state, the phosphorus impurity bond lengths *contract*, while the nitrogen impurity bond lengths *expand*. This result suggests that, in the case of phosphorus, the hole is localized primarily on the p orbital of the P atom; while for N, the p level is below the valence-band maximum and

the hole is instead localized on nearby Se atoms. Thus, as $P_{Se}{}^0 \rightarrow P_{Se}{}^{1-}$, the extra electronic charge goes primarily onto the P atom itself and attracts the positively charged Zn neighbors; while for $N_{Se}{}^0 \rightarrow N_{Se}{}^{1-}$, the extra negative charge goes to the further-neighbor Se atoms and pulls the first-neighbor Zn atoms outward. We will see in Sec. IV D below that this picture is supported by calculations of the defect hole density.

C. Symmetry-breaking distortions

1. Definition of the configuration coordinate

In addition to the breathing relaxation which preserves the tetrahedral (T_d) symmetry of the host material, the impurity can give rise to a Jahn-Teller distortion which reduces the symmetry. As a measure of the significance of this distortion, we define a quantity Q_m to be

$$Q_m = (3z_1 - z_2 - z_3 - z_4)/\sqrt{3}, \tag{1}$$

where z_i is the displacement of the ith Zn neighbor along the bond direction, an outward displacement away from the phosphorus being positive. With this definition, Q_m is zero for symmetric breathing relaxations, and has nonzero values only for symmetry-breaking distortions. For the case of a distortion with C_{3v} symmetry, we define Q to be one unique bond length between the impurity and neighboring Zn atoms and Q' to be the other three, in which case Q_m reduces to $\sqrt{3}(Q - Q')$. The lattice distortion which breaks the original T_d symmetry is illustrated in Fig. 3.

2. P_{Se}

First, we focus on the case of the P impurity in its neutral, -1, and $+1$ charge states, and consider structures in which the P-Zn bond in the [111] direction is lengthened, breaking the T_d symmetry but preserving the trigonal C_{3v} symmetry. We obtained the energy of the system as a function of a configuration coordinate Q

TABLE II. Relaxed bond lengths between impurity (P_{Se} or N_{Se}) and neighboring Zn atoms, under constraint of tetrahedral symmetry. All units are Å. For reference, the bond length of bulk ZnSe is 2.45 Å.

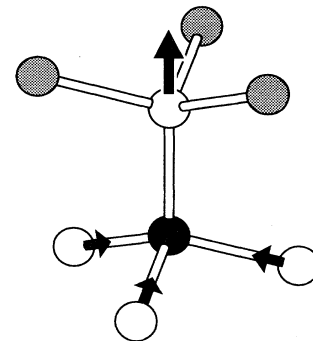| Charge state	P-Zn	N-Zn
-1	2.29	1.96
0	2.33	1.95
$+1$	2.35	1.94

FIG. 3. Illustration of the lattice relaxation due to the Jahn-Teller distortion induced by an impurity. Filled, shaded, and open atoms represent impurity, Se, and Zn atoms, respectively.

which we take to be the length of the P-Zn bond, treating that bond length as a constraint but using the calculated ionic forces to obtain the minimal-energy configuration of the ionic system for the given value of Q. In the process of obtaining the minimal-energy configuration, the P atom and the neighboring Zn atom in the [111] direction were moved together according to the sum of forces on them, preserving the bond length Q, until the sum of forces was negligible, so that the remaining forces are equal and opposite. Since all the other forces are negligible, the remaining force defines the slope of the energy plot as a function of Q. When we determined a stable or metastable structure, we removed the constraint on Q and searched for the configuration in which all the forces are negligible.

For the -1 charge state, a T_d-symmetry structure with breathing relaxations was found to be stable against symmetry-lowering distortions, as expected for a closed-shell structure. However, we found that the Jahn-Teller effect is significant for the neutral state and especially for the 1+ charge state, as shown in Table III. In the neutral state, the P impurity induces a rather small lattice relaxation from the T_d structure due to the Jahn-Teller distortion. The impurity atom increases its bond length with one of its four Zn nearest neighbors by 0.07 Å and decreases it with the other three by 0.03 Å, lowering the crystal structure to C_{3v} symmetry. This relaxation lowered the total energy of the system by only ~ 40 meV relative to that of the T_d-symmetry structure. For the neutral P impurity, the value of Q_m is 0.17 Å.

In the $+1$ charge state, an appreciable lattice relaxation occurred at the P site, with one bond length increased by 0.22 Å and the other three reduced by 0.04 Å, corresponding to a Q_m value of 0.45 Å. This relaxation lowered the energy of the system by 0.15 eV. Figure 4 shows the plot of energies as well as energy derivatives with respect to Q for the case of P_{Se}^{1+}. The point at $Q = 2.35$ Å represents the breathing-relaxed structure with T_d symmetry and the point at $Q = 2.57$ Å indicates the fully relaxed atomic structure with C_{3v} symmetry. We did not find any indications of a second stable or metastable structure at larger Q, for either the neutral or +1 charge state, contrary to previous suggestions.[7]

3. N_{Se}

For the negative charge state of N, as for P, the T_d-symmetry structure was found to be stable against lattice

TABLE III. Stable configurations of P and N impurities in their various charge states. The quantity Q_m is a measure of the lattice distortion due to the Jahn-Teller effect, defined in Eq. (1).

Charge state	P_{Se}		N_{Se}	
	Q_m (Å)	Structure	Q_m (Å)	Structure
-1	0.00	T_d	0.00	T_d
0	0.17	C_{3v}	0.002	$\sim T_d$
$+1$	0.45	C_{3v}	0.003	$\sim T_d$

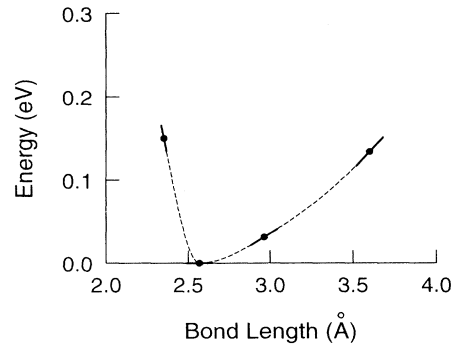FIG. 4. Energy of P_{Se}^{1+} defect vs configuration coordinate Q representing the length of the unique P-Zn bond in the configuration of C_{3v} symmetry. Points represent energies and tangents represent slopes as calculated in the 32-atom cell.

relaxation in the [111] direction. However, we were surprised to find that while the neutral and positive charge states of P assume C_{3v}-symmetry configurations, the corresponding charge states of N assume almost T_d symmetry. That is, the calculated stable configuration of the neutral and positive N states showed such a small Jahn-Teller distortion that it could almost be considered as being within the calculational error bound. Again, the results are summarized in Table III.

Moreover, for the positively charged state of N, our calculation predicts the existence of two minimal-energy structures; the stable one with nearly T_d symmetry as described above, and another metastable structure whose energy is about 0.3 eV higher than the stable one. In this metastable structure, the bond length between the N impurity and one of its nearest-neighbor Zn atoms is greatly increased by 1.34 Å, so that the bond is completely broken. The angle between the axial bond and a basal bond is 98.8°. Since it is 90° for sp^2 and 109.5° for sp^3 bonding, the nitrogen and three of the neighboring zinc atoms are nearly coplanar. We attribute the appearance of a metastable broken-bond configuration for N_{Se}^{1+} but not P_{Se}^{1+} to the fact that the N-Zn bonds are much more highly strained than the P-Zn bonds, as can be seen in Table II. The plot of energies and energy derivatives with respect to Q for the case of N_{Se}^{1+} is

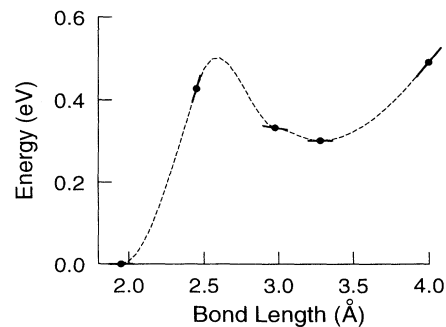
FIG. 5. Energy of N_{Se}^{1+} defect vs configuration coordinate Q representing the length of the unique N-Zn bond in the configuration of C_{3v} symmetry. Points represent energies and tangents represent slopes as calculated in the 32-atom cell.

shown in Fig. 5. The point at $Q = 1.94$ Å represents the atomic structure with nearly T_d symmetry and the point at $Q = 3.28$ Å corresponds to the metastable structure.

The fact that the neutral and positively charged N impurities do not exhibit appreciable Jahn-Teller distortion, while the corresponding states of the P impurity do, is consistent with our interpretation that the acceptor state is much more strongly localized on the impurity p orbital for the case of the P impurity. A brief summary of the defect calculations is given in Table III.

D. Electronic properties of defect states

The structural properties discussed so far have given several indications that the hole state is much more localized to the impurity p orbital for P than for N. Here, we confirm this by direct calculation of the hole densities in the two cases. The hole density plots of P_{Se}^0 and N_{Se}^0 are shown in Fig. 6. (Actually, what is plotted is the electron density in the half-occupied highest valence-band state of the supercell, which is equivalent to the acceptor hole density.) In the case of phosphorus, a substantial portion of the hole density is localized on the p orbital of the P atom; while, in the case of nitrogen, the hole is spread out among second-neighbor and more distant Se atoms. To quantify these features further, we calculated the charges contained within atom-centered spheres around all the atoms. The results are given in Table IV. The sphere radii were 1.96 Å for Se and impurity atoms, and 1.03 Å for Zn atoms. These radii were determined from a bulk ZnSe calculation so that the integrated charge of the highest occupied level inside each sphere would match the values 0.886 for Se and 0.114 for Zn, which are electron charges associated with Se and Zn for the highest level computed from a tight-binding cal-

TABLE IV. Hole densities of P_{Se}^0 and N_{Se}^0. Probability q of finding the hole on the specified subset of atoms is given.

P_{Se}		N_{Se}		Se_{Se}	
Atom	q	Atom	q	Atom	q
P	0.270	N	0.007	Se	0.055
15 Se	0.606	15 Se	0.883	15 Se	0.831
16 Zn	0.130	16 Zn	0.110	16 Zn	0.114

culation. Se_{Se}, which represents bulk ZnSe, is given as a reference to show what the charges would be if the hole were uniformly distributed throughout the supercell.

It can be seen that the hole density on P is enhanced, relative to a uniform distribution; this is to be expected because of the Coulomb attraction of the hole to the acceptor site. (It is not enhanced as much as would be expected for a true deep center, in which case at least half the charge would be expected to reside on the P atom itself.) However, the hole density on N is instead *suppressed*, relative to a uniform distribution. Recalling that the valence-band maximum has primarily anion p character, this can be understood based on the fact that the p level on N is significantly deeper than those on the surrounding Se atoms, giving rise to a strong central-cell correction. Thus the hole avoids the N atom, but is still bound to the impurity by the Coulomb interaction, and therefore spreads itself primarily among the neighboring Se atoms.

This difference in the degree of hole localization is also found to have a strong effect upon the strength of the Jahn-Teller coupling. We calculated the amount of splitting induced between the highest and the next energy levels by a distortion in which the long bond was stretched by 0.072 Å relative to the breathing-relaxed structure, for both P and N defects. (This is the calculated distortion for the P case.) While for P_{Se}^0 the induced splitting was 0.114 eV, for N_{Se}^0 it was only 0.012 eV, or about one order of magnitude smaller. This is clearly a consequence of the fact that the Jahn-Teller split states have so little weight on the impurity and first-neighbor atoms, for the case of N_{Se}^0, and explains the much smaller equilibrium Jahn-Teller distortion found there.

Ideally, it would be desirable to extract the acceptor binding energies directly from the eigenvalues of our supercell calculation. Unfortunately, difficulties in aligning the energy bands of the defective supercell with those of the bulk introduced uncertainties on the order of a few tenths of an eV, which is larger than a typical shallow binding energy. In order to get a rough idea of the acceptor depths, we carried out some simple reference calculations on the same 32-atom supercell using a tight-binding Hamiltonian.[31] The effect of the impurity was modeled by shifting the impurity s and p levels upward or downward on a single site. For P, an upward shift of the on-site energies by about 1.2 eV was sufficient to give good agreement with the *ab initio* charges in Table IV, and also with the calculated dispersion of the defect state. This shift is smaller than the shift of 1.6 eV which we calculated would be needed, within the tight-binding model, to split a localized state off the top of the valence band
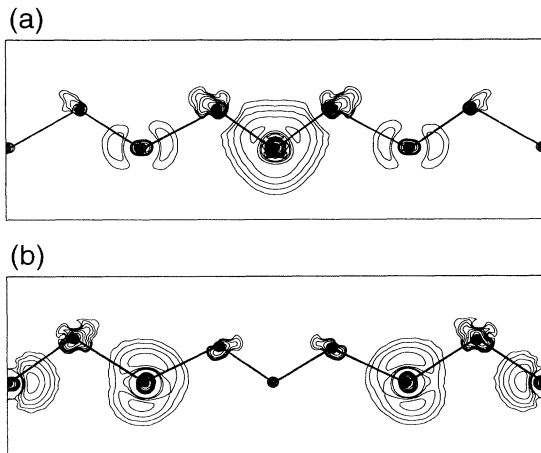
(a)

(b)

FIG. 6. Hole densities for impurities in ZnSe. Central atom is the impurity; other lower atoms are Se, and upper atoms are Zn. For ease of interpretation, plots are given for breathing-relaxed T_d-symmetry structures. (a) Hole density for P_{Se}^0. Hole is mainly localized on P site. (b) Hole density of N_{Se}^0. Hole density is spread around the nearby Se atoms.

in the infinite crystal. A shift large enough to give a lo-
calized state with a binding energy greater than 0.1 eV
in the infinite crystal gave charges and dispersions in the
32-atom cell that were not qualitatively compatible with
the first-principles calculations. For N, a *downward* shift
of about 1.9 eV was found to give a good fit.

Thus the present calculations indicate that $P_{Se}{}^0$ and
$N_{Se}{}^0$ in ZnSe both form shallow acceptors. For the case
of P, the defect level may be near the transition region
to a deep state, but our calculations are not consistent
with an acceptor binding energy greater than ~ 0.1 eV.

V. DISCUSSIONS

Our theoretical result that substitutional nitrogen
forms a shallow acceptor in ZnSe is consistent with the
experimental success[1,2,9] in using nitrogen doping to pro-
duce low-resistivity p-type material. In the effective mass
theory[32] for the acceptor states in ZnSe, the ioniza-
tion energy was calculated to be about 110 meV, show-
ing good agreement for both substitutional nitrogen and
lithium dopants in ZnSe.

Experimentally, two kinds of ionization energies of
phosphorus acceptors in ZnSe have been reported so far.
Reinberg *et al.*[12] studied a strong red emission centered
at 1.91 eV from P-doped ZnSe bulk crystals grown by
the gradient freeze method. A strong EPR signal was
observed in the same samples by Watts *et al.*[11] They
suggested that the origin was a phosphorus ion substi-
tuted at a selenium site (P_{Se}) which induced a Jahn-
Teller distortion to form a deep-acceptor center whose
symmetry was lowered to C_{3v} from T_d by the distor-
tion. The optical activation energy of the deep center was
0.6 eV measured from the infrared quenching of the 1.91
eV emission. Nicholls and Davies[13] carried out optically
detected magnetic-resonance experiments to study the
1.91 eV emission from ZnSe doped with P and Ga grown
by the melt-growth method, and explained the 1.91 eV
photoluminescence (PL) as resulting from a radiative re-
combination between a donor and the P_{Se} center whose
acceptor level lies at about 0.6 eV above the valence-
band maximum (VBM). On the other hand, Kosai *et al.*[9]
studied low temperature PL in P-doped ZnSe grown by
liquid-phase epitaxy (LPE). They observed new donor-
acceptor pair (DAP) bands with the zero-phonon peak
centered at around 2.728 eV. The estimated binding en-
ergy was 84 meV. Aoki *et al.*[14] had grown P-doped ZnSe
using the solution-growth method. They also observed
a dominant DAP emission whose zero-phonon peak is
centered at around 2.72 eV and a very small, deep-lying
emission band. They estimated the binding energy of the
P-related acceptor to be 84 ± 4 meV, similar to the result
of Kosai *et al.*[9]

The present calculation, which predicts the ionization
energy of substitutional P acceptors in ZnSe to be $\lesssim 0.1$
eV, supports the existence of a shallow acceptor state
associated with substitutional P impurity in ZnSe. But
the calculation is not consistent with the results of EPR
experiment by Watts *et al.*[11] on the P-doped ZnSe. They
found that the phosphorus ion substituted at a selenium

site induces a large lattice distortion to form a deep-
acceptor center, by which the bond length between the
phosphorus ion and one of the four nearest-neighbor Zn
atoms was increased by ~ 0.5 Å, and the phosphorus and
other three Zn atoms tend toward an almost coplanar
arrangement. They suggested that the deep-acceptor
center assumed C_{3v} symmetry, lowered from T_d symme-
try due to the distortion. According to our theoretical
calculations, a substitutional P impurity on a Se site in
ZnSe, when it has a configuration of C_{3v} symmetry, forms
a shallow acceptor state whose longer bond length be-
tween the phosphorus and the neighboring Zn atoms is
increased by only ~ 0.07 Å from that of the breathing-
relaxed structure with T_d symmetry.

We have two suggestions to clarify the discrepancy be-
tween our calculation and the EPR experiment. First,
the extraction of the structural parameters and symme-
try from the EPR experiment by Watts *et al.* made
use of assumptions and models which should be con-
firmed by more elaborate experimental and theoretical
investigations. The present calculational methods can
be used to investigate the structure of a substitutional P
impurity in ZnSe without assuming any *a priori* crystal
symmetry. Second, Yao and Okada[10] recently investi-
gated P-doped ZnSe for various P concentrations. The
P-doped ZnSe with various P concentrations was grown
by MBE. From an investigation of the PL spectra, they
found that P formed a shallow acceptor with an activa-
tion energy of 80–92 meV in MBE-grown lightly P-doped
ZnSe, while P formed a deep center with an activation
energy of 0.6–0.7 eV in heavily P-doped ZnSe. It was also
found that the doped P induced point defects in excess
of the doped P atoms. They pointed out that PL spec-
tra of ZnSe which were grown by methods which produce
clear bulk ZnSe [such as LPE (Ref. 33) or solution-growth
method] exhibit small deep-center emissions, while bulk
ZnSe crystals grown by the conventional growth meth-
ods show both the impurity-associated luminescence and
the other deep-center emissions which are attributable to
the self-activated emission and/or Cu-related emission.
Thus they suggested that a shallow P acceptor is com-
monly present in P-doped ZnSe having relatively small
concentrations of point defects, while the deep center is
present in P-doped ZnSe having many point defects. In
conclusion, they proposed a model: a shallow acceptor
level due to unassociated P substituted at a Se site, and
a deep-acceptor level due to the displacement of the P
atom from the tetragonal position. The displacement
would be caused by the presence of many point defects
near the P center, which might make the ZnSe more de-
formable than when there is only a small concentration
of defects.

This suggests the following mechanism of self-com-
pensation of P acceptors substituted at Se sites in ZnSe.
When the doping concentration is low and ZnSe is rela-
tively free of point defects, the substitutional P dopants
form shallow acceptors. But, as the doping concentration
is increased, the deformation induced by the presence of
neighboring defects causes the shallow dopants to trans-
form into distorted deep centers. On the other hand,
our calculation shows that N dopants in ZnSe form a

nearly T_d-symmetry configuration which is stable against a Jahn-Teller distortion, indicating that the N dopant is less likely to be affected by other point defects present nearby. This suggests that N dopants should act as shallow acceptors even when the N doping concentration is increased, thus explaining why N serves as a better dopant than P for p-type ZnSe.

VI. CONCLUSIONS

We have performed pseudopotential total-energy calculations for the electronic and ionic structures of P_{Se} and N_{Se} in ZnSe. Using the ultrasoft pseudopotential scheme, the problematic Zn $3d$ orbitals could be included in the valence band with a modest plane-wave cutoff energy of 25 Ry. Both P_{Se}^{1-} and N_{Se}^{1-} assumed T_d symmetry in their stable structure. We found that N_{Se}^0 forms a shallow acceptor which agrees with experiments. We also identified a shallow acceptor state of P_{Se}^0, but could not find the deep center with C_{3v} symmetry pro-

posed by Watts $et\ al.$ The stable structures of P_{Se}^0 and P_{Se}^{1+} were found to have C_{3v} symmetry, lowered from T_d by a Jahn-Teller distortion. On the other hand, N_{Se}^0 and N_{Se}^{1+} assumed nearly T_d symmetry. This is consistent with our finding that, for P_{Se}, the hole is more localized on the phosphorus site, while for N_{Se}, it is spread around the nearby selenium atoms. It also helps explain why nitrogen is a more robust acceptor dopant than phosphorus. For N_{Se}^{1+}, a metastable state with C_{3v} symmetry was identified, with total energy ~ 0.3 eV higher than that of the stable structure. For P_{Se}^{1+}, no such second metastable structure was found.

ACKNOWLEDGMENTS

[1] J. Qiu, J. M. DePuydt, H. Cheng, and M. A. Haase, Appl. Phys. Lett. **59**, 2992 (1991), and references therein.

[2] M. A. Haase, J. Qiu, J. M. DePuydt, and H. Cheng, Appl. Phys. Lett. **59**, 1272 (1991).

[3] S. Y. Ren, J. D. Dow, and S. Klemm, J. Appl. Phys. **66**, 2065 (1989).

[4] R. W. Jansen and O. F. Sankey, Phys. Rev. B **39**, 3192 (1989).

[5] G. F. Neumark, Phys. Rev. Lett. **62**, 1800 (1989).

[6] D. B. Laks and C. G. Van de Walle, in *Wide Band-Gap Semiconductors*, edited by T. D. Moustakas, J. I. Pankove, and Y. Hamakawa, MRS Symposia Proceedings No. 242 (Materials Research Society, Pittsburgh, 1992); C. G. Van de Walle and D. B. Laks, *ibid.*

[7] D. J. Chadi and K. J. Chang, Appl. Phys. Lett. **55**, 575 (1989); D. J. Chadi, *ibid.* **59**, 3589 (1991).

[8] T. Sasaki, T. Oguchi, and H. Katayama-Yosida, Phys. Rev. B **43**, 9362 (1991).

[9] K. Kosai, B. J. Fitzpatrick, H. G. Grimmeiss, R. N. Bhargava, and G. F. Neumark, Appl. Phys. Lett. **35**, 194 (1979).

[10] T. Yao and Y. Okada, Jpn. J. Appl. Phys. **25**, 821 (1986).

[11] R. K. Watts, W. C. Holton, and M. de Witt, Phys. Rev. B **3**, 404 (1971).

[12] A. R. Reinberg, W. C. Holton, M. de Witt, and R. K. Watts, Phys. Rev. B **3**, 410 (1971).

[13] J. E. Nicholls and J. J. Davies, J. Phys. C **12**, 1917 (1979).

[14] M. Aoki, M. Washiyama, H. Nakamura, and K. Sakamoto, in *Proceedings of the 13th Conference on Solid State Devices, Tokyo, 1981* [Jpn. J. Appl. Phys. Suppl. **21-1**, 11 (1982)].

[15] K. C. Haas and D. Vanderbilt, in *Proceedings of the 18th International Conference on the Physics of Semiconductors*, edited by O. Engstrom (World Scientific, Singapore,

1987), p. 1181.

[16] G. E. Engel and R. J. Needs, Phys. Rev. B **41**, 7876 (1990).

[17] J. L. Martin, N. Troullier, and S.-H. Wei, Phys. Rev. B **43**, 2213 (1991).

[18] A. Continenza, S. Massida, and A. J. Freeman, Phys. Rev. B **38**, 12 996 (1988).

[19] D. Vanderbilt, Phys. Rev. B **41**, 7892 (1990).

[20] K. W. Kwak, R. D. King-Smith, and D. Vanderbilt, Physica B **185**, 154 (1993).

[21] R. D. King-Smith and D. Vanderbilt (unpublished).

[22] J. P. Perdew and A. Zunger, Phys. Rev. B **23**, 5048 (1981).

[23] M. Teter, M. Payne, and D. Allan, Phys. Rev. B **40**, 12 255 (1989).

[24] T. A. Arias, M. C. Payne, and J. D. Joannopoulos, Phys. Rev. Lett. **69**, 1077 (1992).

[25] D. J. Chadi and M. L. Cohen, Phys. Rev. B **8**, 5747 (1973).

[26] D. Vanderbilt and S. G. Louie, Phys. Rev. B **30**, 6118 (1984).

[27] *AIP Handbook* (McGraw-Hill, New York, 1987), p. E-102.

[28] M. S. Hybertsen and S. G. Louie, Phys. Rev. Lett. **55**, 1418 (1985); Phys. Rev. B **34**, 5390 (1986).

[29] X.-P. Li, R. W. Nunes, and D. Vanderbilt, Phys. Rev. B **47**, 10 891 (1993).

[30] E. O. Kane, Phys. Rev. B **31**, 5199 (1985); **31**, 7865 (1985).

[31] W. A. Harrison, Phys. Rev. B **24**, 5835 (1981); **27**, 3592 (1983).

[32] A. Baldereschi and N. O. Lipari, Phys. Rev. B **8**, 2697 (1973).

[33] C. Werkhoven, B. J. Fitzpatrick, S. P. Herko, R. N. Bhargava, and P. J. Dean, Appl. Phys. Lett. **38**, 540 (1981).

[34] B. H. Lee, J. Appl. Phys. **41**, 2982 (1970).

[35] K. Kunc, M. Balkanski, and M. A. Nucimovici, Phys. Status Solidi B **72**, 229 (1975).